



Cite this: *Green Chem.*, 2015, **17**, 1446

Received 30th December 2014,
Accepted 21st January 2015

DOI: 10.1039/c4gc02554g

www.rsc.org/greenchem

Totally atom-economical synthesis of nano/micro structured nickel hydroxide realized by an Ni–O₂ fuel cell†

Junqing Pan,^{*a,d} Meng Yang,^a Yanzhi Sun,^{b,d} Ting Ma,^a Xihong Yue,^a Wei Li^{*c} and Xueliang Sun^d

The conventional syntheses of nickel hydroxide (Ni(OH)₂) produce a large amount of chemical waste because of low atom-economy reactions employed in the processes. Here, we describe a totally atom-economical synthesis of Ni(OH)₂ from nickel metal, water, and oxygen gas (O₂) through a newly designed, membrane-free nickel–oxygen (Ni–O₂) fuel cell. Electricity is also generated as the by-product. The new synthesis method can greatly reduce the pollution to the environment. The as-prepared Ni(OH)₂ has a desired nano/micro structure and exhibits excellent performance as the positive electrode material of nickel–metal hydride batteries.

Introduction

Lately, a tremendous amount of research has been conducted on the development of new electrode materials for advanced batteries, such as nickel–metal hydride (NiMH) and lithium-ion batteries, as the power sources for electric vehicles to reduce the pollution from transportation. However, less attention has been paid to the environmental pollution and energy consumption caused by the synthesis processes of the electrode materials.^{1–5} The widespread usage of the environmentally benign electric vehicles requires the development of green approaches with high atom economy to synthesize the materials. These approaches have a high proportion of reactant atoms incorporated into the desired product.

Nickel hydroxide (Ni(OH)₂) is the active material for the positive electrodes of NiMH batteries^{6–8} and also an important precursor of the positive electrode materials for lithium ion

batteries.^{9–11} It is typically synthesized from the reactions of a nickel salt, *e.g.*, nickel sulfate (NiSO₄), and an alkali, *e.g.*, sodium hydroxide (NaOH).^{12–19} The high purity NiSO₄ is usually synthesized by dissolving metallic nickel (Ni) in a sulfuric acid solution containing nitric acid or hydrogen peroxide as the oxidant in industrial processes.²⁰ The flowchart of a common existing process for the preparation of Ni(OH)₂ is shown in Scheme 1a. This process is atom-uneconomical because a large quantity of unwanted acids and salt are generated from the reaction A1 and reaction A2.^{21,22} The atom economy of this route is 21.6%, as per the calculation shown in the ESI.†

Atom economy is defined as a measure of the proportion of reactant atoms which are incorporated into the desired product of a chemical reaction.²¹ From the view of atom economy, the best route to synthesize Ni(OH)₂ is the direct reaction of metallic Ni, oxygen gas (O₂), and water (H₂O), in which all of the reactants are converted into the product to get a 100% atom economy (Scheme 1b). This reaction is thermodynamically allowed at room temperature with a release of 216.3 kJ mol^{–1} Gibbs free energy. However, it is not kinetically favorable because of two main reasons. One reason is that the Ni metal surface is invariably passivated by a dense nickel oxide film as a barrier for reaction, known as deactivation. The oxide film is formed instantly when the metallic nickel is exposed to air and/or water,²³ or even formed when it is in highly corrosive hydrofluoric acid (HF).²⁴ The other reason is that the O₂ gas has a very low solubility in water, resulting in a very low concentration in the system for reaction. Besides, as the active material for the electrodes in batteries, the synthesized Ni(OH)₂ needs to have a certain ordered crystalline structure to obtain excellent electrochemical activities.

Herein, we describe a 100% atom-economical synthesis of Ni(OH)₂ from Ni metal, water and O₂ based on a newly designed Ni–O₂ fuel cell, which consists of an Ni foam anode, an oxygen cathode electrode with Pt/C catalyst on the carbon paper, and an aqueous electrolyte. The key to realize this route is the activation of the Ni anode. Ni(OH)₂ has been synthesized at a high rate after addressing this challenge and the samples exhibited excellent performances in NiMH batteries.

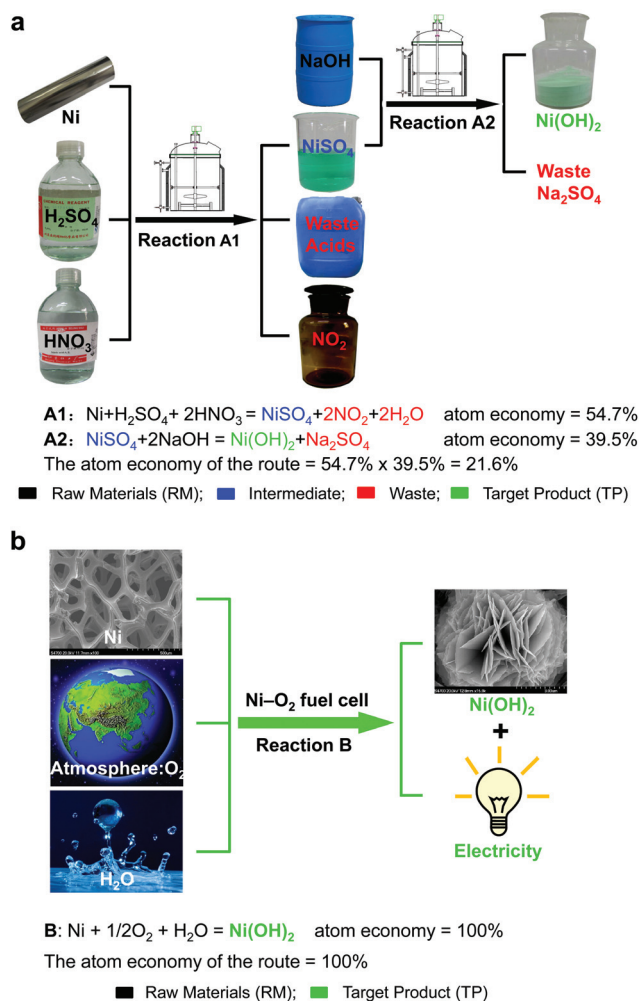
^aState Key Laboratory of Chemical Resource Engineering, Beijing University of Chemical Technology, Beijing 100029, China. E-mail: jqpian@mail.buct.edu.cn

^bNational Fundamental Research Laboratory of New Hazardous Chemicals Assessment and Accident Analysis, Beijing University of Chemical Technology, Beijing 100029, China

^cDepartment of Engineering Technology and Texas Center for Superconductivity, University of Houston, Houston, TX 77204, USA. E-mail: wli23@central.uh.edu

^dDepartment of Mechanical and Materials Engineering, University of Western Ontario, London, ON N6A 5B9, Canada

†Electronic supplementary information (ESI) available. See DOI: 10.1039/c4gc02554g



Scheme 1 Flowcharts for the preparation of Ni(OH)_2 using (a) a conventional process and (b) a nickel–oxygen (Ni-O_2) fuel cell. The calculation for atom economy is in the ESI.†

Results and discussion

Fig. 1 illustrates the schematic of the Ni-O_2 fuel cell, designed to synthesize the nano/micro-structured Ni(OH)_2 . The fuel cell consists of an Ni foam anode, an oxygen cathode, and an aqueous electrolyte. The optimized electrolyte has a pH in the range of 11.30–11.50 (adjusted by NaOH), and is comprised of 0.50 mol L^{-1} sodium sulfate (Na_2SO_4 , 99.5%), 0.60 mol L^{-1} sodium chloride (NaCl , 99.5%), and 2.0 mol L^{-1} aqua ammonia ($\text{NH}_3\cdot\text{H}_2\text{O}$, 25%). The Na_2SO_4 and NaCl were, respectively, used as the supporting electrolyte and activating agent for the Ni anodic dissolution. The $\text{NH}_3\cdot\text{H}_2\text{O}$ was used as the complexation agent. The selection and optimization of this composition will be thoroughly discussed hereunder.

The Ni(OH)_2 is synthesized by electrochemical reactions and a complexation–precipitation reaction as shown in eqn (1)–(4). In the cell, the Ni foam anode undergoes an electro-oxidation reaction, or anodic dissolution, to produce

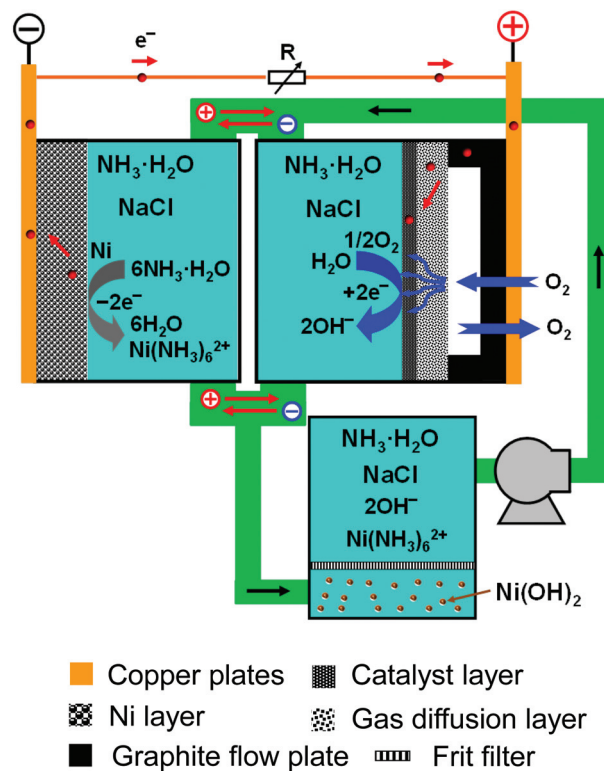
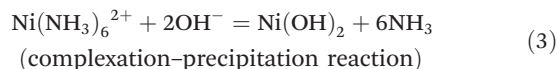
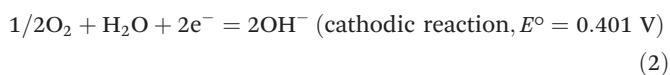
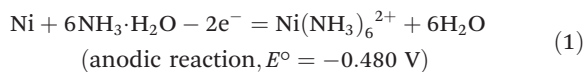
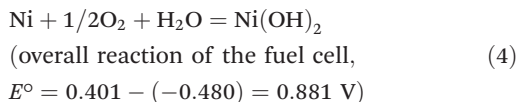


Fig. 1 Diagram of the Ni-O_2 fuel cell. The diffusion layer is a carbon paper (TGP-H-060, Toray) coated with carbon black (Vulcan 72R, Cabot). The cathode catalyst is platinum nanoparticles supported on carbon black (40 wt% Pt/C, HiSPEC™ 4000, Johnson Matthey).

$\text{Ni(NH}_3)_6^{2+}$ and releases electrons (eqn (1)). The electrons travel through the external electric circuit, do electric work, and arrive at the cathode. O_2 is fed into the cathode, where it is electro-chemically reduced with water and the electrons from the anode to produce OH^- ions (eqn (2)). Though the anode and cathode compartments are separated to protect the freshly produced $\text{Ni(NH}_3)_6^{2+}$ and OH^- ions from instant combination, the internal circuit is formed by the transport of $\text{Ni(NH}_3)_6^{2+}$ and OH^- ions through the pipe joints before and after the compartments. The two electro-chemical reactions of eqn (1) and (2) and the chemical reaction of eqn (3) combine into the overall reaction of the fuel cell (eqn (4)). The positive standard potential of 0.881 V means that the reaction of metallic Ni, O_2 , and water to synthesize Ni(OH)_2 can spontaneously occur in the Ni-O_2 fuel cell.





As the reactions of eqn (1) and (2) continue, the concentration of $\text{Ni}(\text{NH}_3)_6^{2+}$ and OH^- ions increases to the saturation points for the appearance of the nuclei of $\text{Ni}(\text{OH})_2$. They move along with the flow of electrolyte in the pipe system and enter the electrolyte tank where the $\text{Ni}(\text{OH})_2$ nuclei undergo crystal nucleation and growth to micro powders.¹⁹ It needs to be mentioned that both the pipe system and the tank are heated to the fuel cell temperature to avoid the precipitation of $\text{Ni}(\text{OH})_2$ at a lower temperature. The small particles can dissolve through the complexation dissolution process and then re-precipitate on the surface of the large $\text{Ni}(\text{OH})_2$ particles. This precipitation-complexation dissolution is a dynamic process, which helps to generate spherical $\text{Ni}(\text{OH})_2$ powders with the desired nano/micro structure/morphology for NiMH batteries.¹⁹

The formed $\text{Ni}(\text{OH})_2$ powders reside in the tank by the block of a frit filter. The filtrate is pumped back into the fuel cell for the consecutive reactions when the concentrations of $\text{Ni}(\text{NH}_3)_6^{2+}$ and OH^- are at the saturation point. These concentrations increase again through the reactions in the cell and $\text{Ni}(\text{OH})_2$ nuclei are produced by the reaction of eqn (3) in the existing pipe system and collected in the tank to form $\text{Ni}(\text{OH})_2$ powders.

Activation of the electrodes needs to be investigated to improve the performance of the Ni–O₂ fuel cell and thus to produce more $\text{Ni}(\text{OH})_2$. The oxygen cathode has been extensively investigated as it is a common cathode for low temperature fuel cells, such as proton exchange membrane fuel cells and direct methanol fuel cells, *etc.* The Ni anode, on the contrary, has not been reported as the anode for a fuel cell and thus it is investigated herein for the newly proposed Ni–O₂ fuel cell. Ni metal is known to be easily passivated by forming oxides in the environment.²³ When it is used as an anode, the passivation becomes more severe owing to more oxide produced by oxidation reactions, leading to a significant increase in the polarization of its anodic dissolution. To make the new route feasible to synthesize $\text{Ni}(\text{OH})_2$, the Ni anode needs to be prevented from passivation and kept activated during the anodic dissolution process. Here we demonstrate the investigation with an Ni foam anode rather than a Ni plate anode because the Ni foam anode produced a larger current with a larger surface area, as shown in Fig. S1.† Study on activation with an Ni plate anode will be conducted in the future.

The effect of the $\text{NH}_3\cdot\text{H}_2\text{O}$ concentration on the anodic polarization is shown in Fig. 2a. As the concentration increases, the anodic reaction (eqn (2)) moves forward, resulting in the increase in the anodic current. It also suppresses the combination of $\text{Ni}(\text{NH}_3)_6^{2+}$ and OH^- to produce $\text{Ni}(\text{OH})_2$ (eqn (3)) on the surface, by which the anode surface passivation by the $\text{Ni}(\text{OH})_2$ is mitigated. The anodic current density reaches the maximum value of 9.0 mA cm^{-2} , equivalent to an

$\text{Ni}(\text{OH})_2$ production rate of $15.6 \text{ mg h}^{-1} \text{ cm}^{-2}$, at 2.0 mol L^{-1} concentration of $\text{NH}_3\cdot\text{H}_2\text{O}$ and hardly increases further with the concentration.

It is known that halogen ions can destruct metal oxide films and an applicable example was demonstrated by activating aluminum, an active metal similar to Ni, as an effective reducing agent for wet-chemical synthesis through the addition of halogen ions.²⁵ Further activation of the Ni anode was conducted in this study by comparing the effects of different halogen ions. As shown in Fig. 2b, the anodic current densities with the presence of halogen ions are much larger than the current densities measured without halogen ions. The field emission – scanning electron microscope (FE-SEM) images of the Ni anode before and after anodic dissolution in Fig. 2c and 2d show the evidence of the surface corrosion. Moreover, the anodic current densities decrease in the order of $\text{Cl}^- > \text{Br}^- > \text{I}^-$, which can be explained by the fact that a smaller ion can more easily penetrate the oxide film.²⁵ The anodic polarization with F^- ions is exceptional to this trend owing to three reasons: the F^- ions remain hydrated when attacking the passive oxide film, the formed NiF_2 contributes to the passivation film on the Ni surface, and NiF_2 has a lower solubility than NiCl_2 .^{23,26–28}

The Cl^- concentration was then optimized for the anodic dissolution of the Ni anode. Fig. 2e shows that the anodic current substantially increases as the Cl^- concentration increases from 0.10 to 0.60 mol L^{-1} . Further increase in the concentration does not significantly increase the current, suggesting that the activation process with 0.60 mol L^{-1} of Cl^- is fast enough. The maximum current density is 90.6 mA cm^{-2} , about 10 times of that without the presence of Cl^- ions.

Fig. 3 shows the polarization and power curves of an Ni–O₂ fuel cell with a nickel foam anode and an aqueous electrolyte (pH = 11.30–11.50, adjusted by NaOH) of $0.50 \text{ mol L}^{-1} \text{ Na}_2\text{SO}_4$, $2.0 \text{ mol L}^{-1} \text{ NH}_3\cdot\text{H}_2\text{O}$, and $0.60 \text{ mol L}^{-1} \text{ NaCl}$. It is easily seen that the maximum specific power of 15 mW cm^{-2} is generated at a voltage of 0.3 V and current density of 50 mA cm^{-2} . The fuel cell operates stably as shown in Fig. S2,† which is beneficial for the synthesis of $\text{Ni}(\text{OH})_2$ with high quality. Because the fuel cell is designed for material synthesis, a large current needs to be chosen instead of a large power. We chose a current of 80% maxima (40 mA cm^{-2}) for synthesizing $\text{Ni}(\text{OH})_2$, equivalent to an $\text{Ni}(\text{OH})_2$ production rate of $68.6 \text{ mg h}^{-1} \text{ cm}^{-2}$.

Fig. 4a shows the XRD pattern of the synthesized $\text{Ni}(\text{OH})_2$ sample. The XRD peaks located at 2-theta degrees of 19.42° , 33.24° , 38.70° , 52.27° and 59.30° , are corresponding to the reflections of the $\beta\text{-Ni}(\text{OH})_2$ crystalline planes of (001), (100), (101), (102) and (110) (standard XRD pattern: JCPDS #14-0117), respectively. The sample is rather uniformly spherical (*ca.* $10 \mu\text{m}$ in diameter) as shown by the low magnification FE-SEM image in Fig. 4b. The spherical particles have a flower structure at the micrometer scale with thin nano-plates crossed and stacked, as shown by the high magnification FE-SEM image in Fig. 4c. The loose channels between the nano-plates help the migration of protons and electrons, thus enhancing the electrochemical performances of the $\text{Ni}(\text{OH})_2$.¹⁹

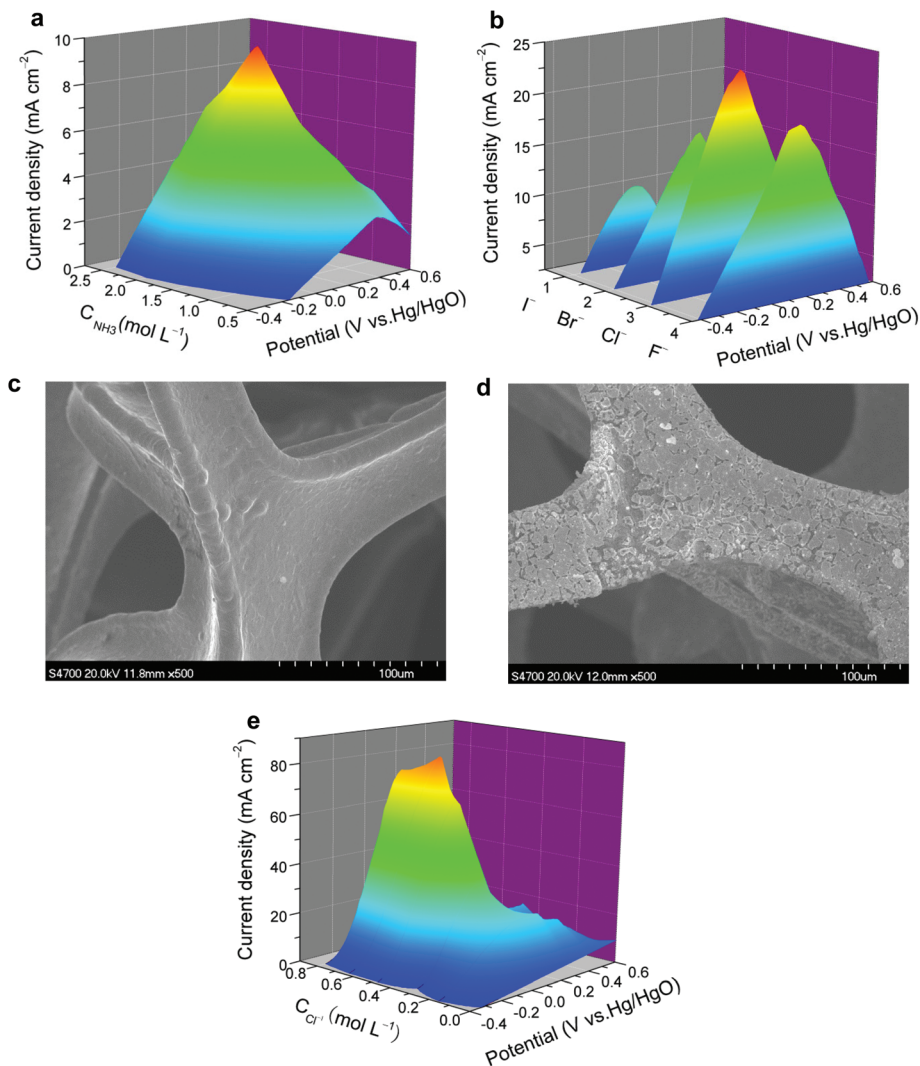


Fig. 2 Anode polarization curves with (a) different concentrations of $\text{NH}_3\cdot\text{H}_2\text{O}$ and $0.50 \text{ mol L}^{-1} \text{ Na}_2\text{SO}_4$, and (b) different halogen ions (0.50 mol L^{-1} , $0.50 \text{ mol L}^{-1} \text{ Na}_2\text{SO}_4$, and $2.0 \text{ mol L}^{-1} \text{ NH}_3\cdot\text{H}_2\text{O}$; FE-SEM images of the Ni foam anode (c) before and (d) after reaction; and (e) anode polarization curves with different concentrations of Cl^- ions, $0.50 \text{ mol L}^{-1} \text{ Na}_2\text{SO}_4$, and $2.0 \text{ mol L}^{-1} \text{ NH}_3\cdot\text{H}_2\text{O}$. All of the electrolytes had a pH in the range of 11.30–11.50. The potential scanning rates were 2 mV s^{-1} and the temperature was $55 \text{ }^\circ\text{C}$.

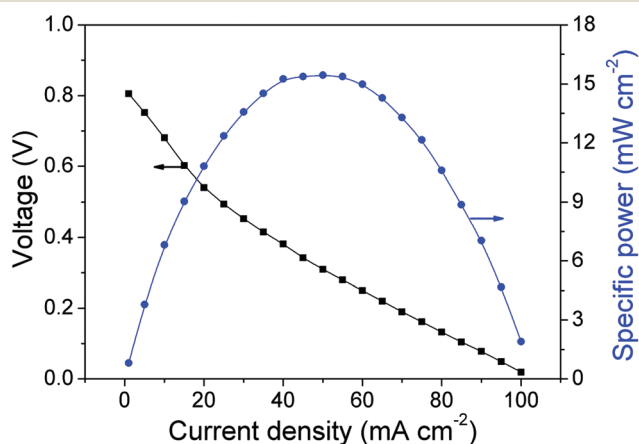


Fig. 3 Polarization and power curves of the Ni– O_2 fuel cell. The fuel cell operated with a nickel foam anode and an aqueous electrolyte (pH = 11.30–11.50, adjusted by NaOH) of $0.50 \text{ mol L}^{-1} \text{ Na}_2\text{SO}_4$, $2.0 \text{ mol L}^{-1} \text{ NH}_3\cdot\text{H}_2\text{O}$, and $0.60 \text{ mol L}^{-1} \text{ NaCl}$ at $55 \text{ }^\circ\text{C}$.

The electrochemical performances of the synthesized nano/micro-structured $\beta\text{-Ni}(\text{OH})_2$ sample were investigated by charge/discharge and cyclic voltammetry (CV) experiments. The charge/discharge experiments were carried out at very high current densities of 1000, 2000, and 5000 mA g^{-1} . After the activation period, the charge/discharge curves at the 10th cycle in Fig. 4d show that the discharge capacities of the $\beta\text{-Ni}(\text{OH})_2$ electrode are higher than 260 mAh g^{-1} at current densities of 1000, 2000, and 5000 mA g^{-1} , which are comparable to the capacities of the state-of-the-art $\beta\text{-Ni}(\text{OH})_2$ samples prepared by conventional methods.^{15,19} After 350 cycles, the discharge specific capacities reduce by 7.6%, 8.3%, and 9.2%, respectively, at current densities of 1000, 2000, and 5000 mA g^{-1} as shown in Fig. S3a.† As for these high current densities, the results mean that the synthesized $\beta\text{-Ni}(\text{OH})_2$ samples have excellent cycling stability.^{15,19} Besides, the CV curves of the synthesized $\beta\text{-Ni}(\text{OH})_2$ samples in Fig. S3b.† show about a

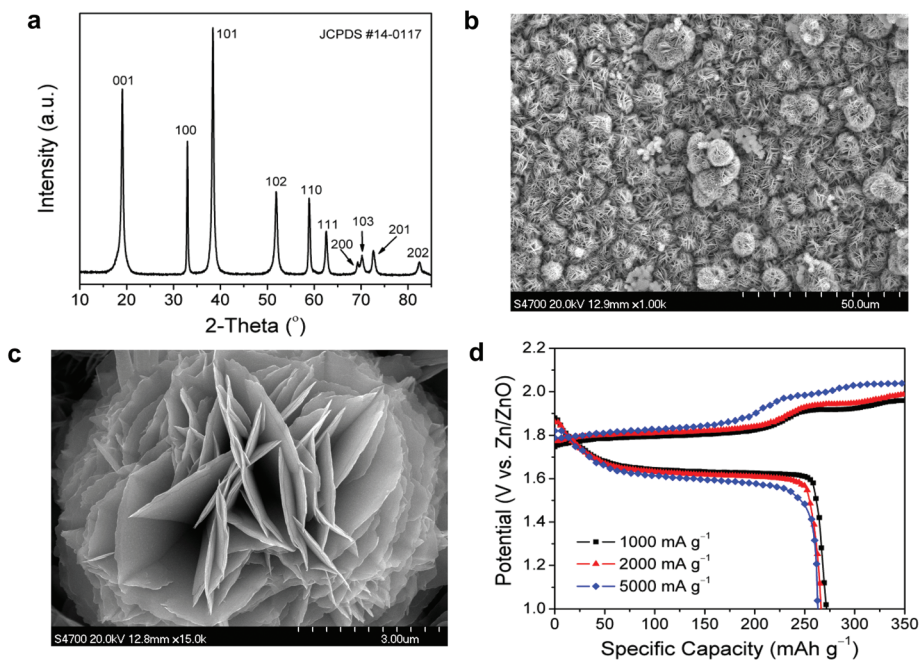


Fig. 4 (a) X-ray diffraction pattern, (b) low magnification and (c) high magnification field emission-scanning electron microscope (FE-SEM) images of the nano/micro structured β -Ni(OH)₂ sample synthesized in an Ni–O₂ fuel cell at 40 mA cm⁻² at 55 °C, (d) its charge/discharge curves in an electrochemical cell with a three-electrode configuration. The fuel cell employed a nickel foam anode and an aqueous electrolyte (pH = 11.30–11.50, adjusted by NaOH) of 0.50 mol L⁻¹ Na₂SO₄, 2.0 mol L⁻¹ NH₃·H₂O, and 0.60 mol L⁻¹ NaCl.

300 mV difference between the positions of oxidation peaks and reduction peaks. This indicates excellent reversibility of the synthesized β -Ni(OH)₂ samples.^{15,19}

Conclusions

This study demonstrates the feasibility of a 100% atom-economical route for the synthesis of Ni(OH)₂ from nickel metal, water, and O₂ based on a newly designed membrane-free Ni–O₂ fuel cell. The synthesized Ni(OH)₂ has the desired nano/micro structure for the positive electrode material and exhibits excellent performance in NiMH batteries. The activation of the Ni anode by the complexation of NH₃·H₂O and Ni²⁺ as well as the destruction of the protective oxide film by Cl⁻ ions is the key to the success. This green synthesis is potentially applicable for the syntheses of other metal hydroxides using a metal–O₂ fuel cell. The metal should have a lower standard electrode potential than that of oxygen gas and a protective oxide film on the surface so that it can be stable in water. Appropriate additives thus need to be figured out to activate the metal for anodic dissolution.

Experimental

The chemicals sodium sulfate (Na₂SO₄, 99.5%), sodium chloride (NaCl, 99.5%), aqua ammonia (NH₃·H₂O, 25%), sodium hydroxide (NaOH, 99%) and hydrochloric acid (HCl, 37%) were

all of analytical reagent grade, which were purchased from Beijing Chemical Factory in China and used as received.

Activation of Ni anode

The study of the activation of the Ni anode was carried out in an electrochemical cell with a three-electrode configuration. An Ni foam (300 g m⁻² in area density, 1 mm in thickness, and 99.5% in purity, Heze Tianyu Technology Company), an Ni wire (99.9% in purity, Beijing Zhongjin Yan New Material Technology), and an Hg/HgO electrode were, respectively, used as the working electrode, the counter electrode, and the reference electrode. The Ni working electrode was pretreated by rinsing with acetone to remove the grease, immersion into a 3.0 mol L⁻¹ HCl solution for 10 min to eliminate the passivation film (an oxide film on the surface) and rinsing again with deionized water. To characterize the activation of the Ni anodes under different conditions of temperature, concentrations of ammonia and halogen ions, the potentiodynamic polarization experiments were performed at a scanning rate of 2.0 mV s⁻¹ between -0.30 V and 0.60 V on a CSU-300 electrochemical workstation (Wuhan Corrtest Instrument). In all of these electrochemical experiments, 0.50 mol L⁻¹ Na₂SO₄ was used as the supporting electrolyte.

Ni–O₂ fuel cell and 100% atom-economical synthesis of Ni(OH)₂

The Ni–O₂ fuel cell consisted of an Ni foam anode (25 mm × 20 mm), an oxygen cathode made of a carbon paper (25 mm × 20 mm, TGP-H-060, Toray) with a carbon black (Vulcan 72R,

Cabot) loading of 0.5 mg cm^{-2} and a catalyst loading of 1.2 mg cm^{-2} (40 wt% Pt/C, Johnson Matthey), and an aqueous electrolyte containing $0.50 \text{ mol L}^{-1} \text{ Na}_2\text{SO}_4$, $2.0 \text{ mol L}^{-1} \text{ NH}_3\cdot\text{H}_2\text{O}$, and $0.60 \text{ mol L}^{-1} \text{ NaCl}$. The nickel foam anode was pretreated as in the study for Ni anode activation. The distance between two electrodes was 20 mm. The polarization curves and stability curves of the fuel cell were, respectively, recorded potentiostatically and galvanostatically on a battery test station (LAND-CT2001A).

The synthesis of $\text{Ni}(\text{OH})_2$ was carried out in an $\text{Ni}-\text{O}_2$ fuel cell with a nickel foam anode and under the optimized conditions of $55 \text{ }^\circ\text{C}$ and an aqueous electrolyte (pH = 11.30–11.50, adjusted by NaOH) of $0.50 \text{ mol L}^{-1} \text{ Na}_2\text{SO}_4$, $2.0 \text{ mol L}^{-1} \text{ NH}_3\cdot\text{H}_2\text{O}$, and $0.60 \text{ mol L}^{-1} \text{ NaCl}$. The total amount of electrolyte was 500 mL and it was circulated between the fuel cell and a sealed tank at a rate of 40 mL min^{-1} using a peristaltic pump during the operation of the fuel cell. The fuel cell operated galvanostatically with a current density of 40 mA cm^{-2} . The synthesized $\text{Ni}(\text{OH})_2$ nuclei were carried by the flow of the electrolyte into the tank and stayed there due to the block of a glass frit filter with *ca.* $3 \text{ }\mu\text{m}$ nominal pore size. In the tank, the $\text{Ni}(\text{OH})_2$ nuclei grow and form the nano/micro structure.

Physical characterizations

The powder X-ray diffraction (XRD) patterns of the synthesized $\text{Ni}(\text{OH})_2$ were obtained on a Rigaku D/max2500VB2+/PC diffractometer with Cu K α radiation ($\lambda = 0.15418 \text{ nm}$, 40 kV, 200 mA) at a scanning rate of $10^\circ \text{ min}^{-1}$ with a step size of 0.02° (0.12 s per step). A field emission-scanning electron microscope (FE-SEM, Hitachi S4700) was used to characterize the morphology of the Ni anodes and the synthesized $\text{Ni}(\text{OH})_2$ samples. The discharged Ni anodes were taken out from the fuel cell and quickly placed in an N_2 filled container to avoid oxidation by air before FE-SEM characterization.

Electrochemical characterizations of the synthesized $\text{Ni}(\text{OH})_2$

The mixture of as-prepared $0.20 \text{ g Ni}(\text{OH})_2$ and 0.050 g expanded graphite powders (OER-CX200, China Sciences Hengda Graphite) was ground with an agate pestle and mortar. The mixture was further ground with an amount of 5 wt% polytetrafluoroethylene (PTFE) suspension (60 wt%, Guangzhou Songbai Chemicals Company) and then fed into a roller press to fabricate a film $80 \text{ }\mu\text{m}$ in thickness. This film was pressed on a piece of Ni foam to obtain the working electrode. A three-electrode configuration was built with this working electrode, a Zn/ZnO electrode (home-made) as the reference electrode,¹⁹ and a Ni wire as the counter electrode. The three electrodes sit still in an aqueous electrolyte ($6.0 \text{ mol L}^{-1} \text{ KOH}$) for 3 h to reach equilibrium. The charging/discharging experiments and cyclic voltammetry experiments were, respectively, carried out on a battery test station (LAND-CT2001A) and a CSU-300 electrochemical workstation (Wuhan Corrtest Instrument).¹⁹ The discharge specific capacity was calculated based on the mass of nickel hydroxide in the electrode.

Conflict of interest

The authors declare no competing financial interests.

Acknowledgements

The work at Beijing University of Chemical Technology (BUCT, China) was supported by the State Key Program of National Natural Science of China (no. 21236003), National Natural Science Foundation of China (no. 21476022) and Beijing Higher Education Young Elite Teacher Project (YETP0509).

References

- 1 P. Bocchetta, M. Santamaria and F. Di Quarto, *Electrochem. Commun.*, 2007, **9**, 683–688.
- 2 F. Y. Cheng, J. Chen, X. L. Gou and P. W. Shen, *Adv. Mater.*, 2005, **17**, 2753–2756.
- 3 S. Zhu, H. Zhou, T. Miyoshi, M. Hibino, I. Honma and M. Ichihara, *Adv. Mater.*, 2004, **16**, 2012–2017.
- 4 Y. Sun, X. Hu, W. Luo and Y. Huang, *ACS Nano*, 2011, **5**, 7100–7107.
- 5 Y. Gu, D. Chen and X. Jiao, *J. Phys. Chem. B*, 2005, **109**, 17901–17906.
- 6 M. Geng and D. O. Northwood, *Int. J. Hydrogen Energy*, 2003, **28**, 633–636.
- 7 M. Casas-Cabanas, J. Canales-Vázquez, J. Rodríguez-Carvajal and M. R. Palacín, *J. Am. Chem. Soc.*, 2007, **129**, 5840–5842.
- 8 D. M. MacArthur, *J. Electrochem. Soc.*, 1970, **117**, 422–426.
- 9 Y.-K. Sun, S.-T. Myung, M.-H. Kim, J. Prakash and K. Amine, *J. Am. Chem. Soc.*, 2005, **127**, 13411–13418.
- 10 W. Luo, X. Li and J. R. Dahn, *Chem. Mater.*, 2010, **22**, 5065–5073.
- 11 K. M. Shaju and P. G. Bruce, *Adv. Mater.*, 2006, **18**, 2330–2334.
- 12 K. C. Ho and J. Jorné, *J. Electrochem. Soc.*, 1990, **137**, 149–158.
- 13 M. J. Avena, M. V. Vazquez, R. E. Carbonio, C. P. Pauli and V. A. Macagno, *J. Appl. Electrochem.*, 1994, **24**, 256–260.
- 14 M. Akinc, N. Jongen, J. Lemaître and H. Hofmann, *J. Eur. Ceram. Soc.*, 1998, **18**, 1559–1564.
- 15 F.-S. Cai, G.-Y. Zhang, J. Chen, X.-L. Gou, H.-K. Liu and S.-X. Dou, *Angew. Chem., Int. Ed.*, 2004, **43**, 4212–4216.
- 16 Y. Li, W. Li, S. Chou and J. Chen, *J. Alloys Compd.*, 2008, **456**, 339–343.
- 17 P. Jeevanandam, Y. Kolytyn and A. Gedanken, *Nano Lett.*, 2001, **1**, 263–266.
- 18 M. Vidotti, C. van Greco, E. A. Ponzio and S. I. Córdoba de Torresi, *Electrochem. Commun.*, 2006, **8**, 554–560.
- 19 X. Yue, J. Pan, Y. Sun and Z. Wang, *Ind. Eng. Chem. Res.*, 2012, **51**, 8358–8365.
- 20 Univertical Corporation, <http://www.univertical.cn/en/products03.htm>, (accessed Oct. 2014).

- 21 B. Trost, *Science*, 1991, **254**, 1471–1477.
- 22 B. R. Reddy, C. Parija and P. V. R. B. Sarma, *Hydro-metallurgy*, 1999, **53**, 11–17.
- 23 J. L. Trompette, L. Massot and H. Vergnes, *Corros. Sci.*, 2013, **74**, 187–193.
- 24 Y. Li, X. Fan, N. Tang, H. Bian, Y. Hou, Y. Koizumi and A. Chiba, *Corros. Sci.*, 2014, **78**, 101–110.
- 25 W. Li, T. Cochell and A. Manthiram, *Sci. Rep.*, 2013, **3**, 1229.
- 26 N. Hackerman, E. S. Snively Jr. and L. D. Fiel, *Electrochim. Acta*, 1967, **12**, 535–551.
- 27 B. Löchel, H. H. Strehblow and M. Sakashita, *J. Electrochem. Soc.*, 1984, **131**, 522–529.
- 28 B. P. Löchel and H. H. Strehblow, *J. Electrochem. Soc.*, 1984, **131**, 713–723.